Research on Engineering Structures & Materials
www.jresm.org
Research Group

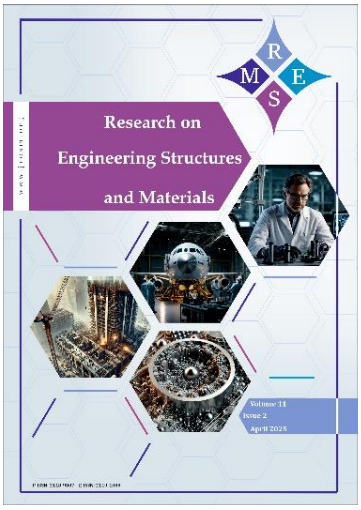

Experimental and numerical free vibration analysis of orthotropic composite plates reinforced with Al_2O_3

Dunia Abd Al-Latteef, Mohsin A. Al-Shammari, Emad Q. Hussein

Online Publication Date: 10 January 2026

URL: http://www.jresm.org/archive/resm2026-1299ic1027rs.html
DOI: http://dx.doi.org/10.17515/resm2026-1299ic1027rs

Journal Abbreviation: *Res. Eng. Struct. Mater.*

To cite this article
Al-Latteef D A, Mohsin Al-Shammari A, Hussein E Q. Experimental and numerical free vibration analysis of orthotropic composite plates reinforced with Al_2O_3. *Res. Eng. Struct. Mater.*, 2026; 12(2): 1115-1125

Research on Engineering Structures & Materials
www.jresm.org

Research Article

Experimental and numerical free vibration analysis of orthotropic composite plates reinforced with Al_2O_3

Dunia Abd Al-Latteef [*,1], Mohsin A. Al-Shammari [2,a], Emad Q. Hussein [1,b]

[1]*Department of Mechanical Engineering, University of Karbala, Karbala, Iraq*
[2]*Department of Mechanical Engineering, University of Baghdad, Baghdad, Iraq*

Article Info

Article History:

Received 27 Oct 2025
Accepted 01 Jan 2026

Keywords:

Free vibration;
Composite plate;
Alumina;
Natural frequency;
Classical laminate theory

Abstract

The dynamic behavior of composite structures is crucial for aerospace and automotive applications where weight reduction and vibration control are essential. This study investigates the free vibration characteristics of orthotropic composite plates reinforced with aluminum oxide (Al_2O_3) particles. Limited research exists on the combined effect of Al_2O_3 reinforcement percentages and fiber orientation on the dynamic properties of composite plates. The study aims to analyze the influence of varying Al_2O_3 content (2%, 5%, and 8% by weight) on the natural frequencies of glass fiber-reinforced PMMA composite plates with different stacking sequences. The study employs Classical Laminate Theory (CLT) with Rayleigh-Ritz method for analytical modeling, assuming thin plate theory (Kirchhoff), neglecting shear deformation, and considering simply supported boundary conditions. Finite Element Method (FEM) using ANSYS Workbench with SHELL181 elements validates the analytical results. Experimental verification uses impact hammer testing with accelerometer measurements. The 8% Al_2O_3 reinforcement showed optimal mechanical properties with the highest natural frequency (104.51 Hz) achieved by (90°, 30°, 45°, 30°, 90°) stacking sequence. Analytical-numerical correlation showed excellent agreement with discrepancies below 3% for most modes, while experimental validation confirmed model accuracy with errors ranging from 0.03% to 3.69%.

1. Introduction

Uncontrolled vibrations lead to resonance and potential structural damage, so researchers focus on modeling the behavior of these plates and understanding the effect of particle reinforcement on dynamic properties [1-3]. Merdaci et al. [4] analyzed the vibrations of aluminum-alumina functional gradient plates from manufacturing, using higher order shear deformation theory and Navier's solution. The results were validated by comparing them with the literature and showing the effect of gradient coefficient, pore size and distribution, and dimensional ratios on normal frequencies [4]. Navaneeth et al. [5] examined free damping vibrations of woven fiberglass composite panels and a hand-molded epoxy matrix, with an assessment of tensile and bending properties according to ASTM standards, and natural frequency analysis using FFT and an accelerator with impact hammer; the results showed good compatibility with NASTRAN simulation and increased frequency response with increasing the number of layers [5]. Al-Shablle et al. [6] used theoretical, experimental and numerical analysis to study the vibrations of the nano-coated composite structural plate (SiO_2 epoxy and Al_2O_3 epoxy) at 0–2.5% volumetric ratios, showing an optimal increase in Young's modulus (up to 56%) and natural frequency (up to 24.5%) with different densities, with analytical-numerical compatibility with deviation of ≤3% [6].

*Corresponding author: dralihadi841@gmail.com
[a]orcid.org/0000-0002-2372-4840; [b]orcid.org/0000-0001-8643-2143
DOI: http://dx.doi.org/10.17515/resm2026-1299ic1027rs

Vasara et al. aimed to determine the natural frequencies of circular and annular plates with functional and porous gradient according to distributions (uniform, O-shape, X-shape), with modeling of mechanical properties via the Voght model and the distribution by power law, using the first shear deformation theorem, Hamilton's principle and a solution by differential quadrature method [7]. Saidi et al. [8] analyzed the free vibrations of plates with a functional gradient and porosity composed of aluminum (Al) and alumina (Al_2O_3) supported by an elastic medium, using the new shear deformation theory and the Winkler–Patrick two-coefficient model, and solving Navier's equations; the results showed the effect of gradient coefficient, degree of porosity and base constants on natural frequencies [8]. Venkatalakshmi et al. [9] proposed a synchronous field (CDF) method to analyze the free vibration of ceramic and metal gradient plates under proven and abstract edge conditions, with the distribution of material properties across thickness by force law, and the use of multiple nominal functions to obtain frequency coefficients and verify them by comparing them with the literature [9]. Li et al. [10] presented an accurate solution method for the analysis of the static response and free vibration of a rectangular plate with functional hierarchy according to the Reisner–Mingelen theorem with general edge conditions, with the distribution of material properties across thickness by force law and estimation by Vogt and Morri-tanka models, and improved Fourier series verification [10].

Tavadi et al. [11] analyzed the properties of epoxy compounds reinforced with erica fibers with the addition of alumina molecules (0-8%). The results showed that the 8% sample excelled in tensile tolerance (23 MPa), stiffness (81 Shore D), and impact resistance (180 J/m^2) due to uniform distribution and good bonding, supporting its use in lightweight engineering applications [11]. Han et al. [12] studied the nonlinear vibrations of plastic reinforced carbon fiber composite panels (CFRP) using machine learning techniques. A highly accurate predictive model (R^2=0.96) was developed to analyze the effect of multiple factors such as load levels, geometric dimensions, and boundary conditions on nonlinear frequency ratio. This model contributes to a better understanding of the dynamic vibration behavior of these materials, supporting the assessment of the robustness of CFRP structures and extending their service life in various engineering applications [12]. Mawardi et al. [13] investigated the effect of the addition of micro-aluminum oxide (Al_2O_3) molecules on the properties of pineapple fiber compounds reinforced with different polymeric matrices (epoxy and unsaturated polyester). The results showed that increasing the ratio of Al_2O_3 (up to 15% by weight) enhances stiffness, bending strength and resistance to water absorption, but reduces tensile strength. Epoxy compounds excelled in tensile strength and thermal stability, while polyester excelled in hardness and density of water. The uniform distribution of molecules contributed to the improved adhesion of the fibers to the polymeric matrix [13].

Despite the progress made, there are still points worth exploring further, which will therefore be highlighted in this study: using different percentages of Al_2O_3 and their effect on the dynamic analysis of the orthotropic composite plates. Study the effect of different percentages of Al_2O_3 through engineering simulations using FEM. In this study, the focus is on research that includes modeling methods used, techniques and methods of enhancing Al_2O_3 as weight ratio or functional distribution across thickness, type of plates studied, panel geometry, edge installation conditions, and the main findings of each researcher. We also discuss the importance of these studies for practical applications in areas such as aviation, automobiles and smart systems, and what new research can add in this field.

2. Materials and Testing Methods

2.1 Materials

The materials used in this study are presented in the following: E-Glass fibers: Long wires (roving) were used as structural reinforcement, PMMA mixture in a ratio of 80:20 (polymethyl methacrylate) was used as the matrix resin. Hardener: A powder added by 2% by weight of the resin to accelerate the hardening process of the resin. Aluminum oxide: powder added as a 2%, 5%, and 8% distributed additive. Polyvinyl Alcohol (PVA): A PVA bag or wrap was used to prevent resin from leaking while applied to the fibers, and ensures a smooth finish surface for the samples. The mechanical properties of the materials used are shown in Table 1. A gypsum mold of dimension (25×35×5 cm3) was used as shown in (Fig. 1).

Table 1. Mechanical properties of the used materials.

Material	Elastic modulus (GPa)	Density (g/cm^3)	Volume fraction (%)	Poisson's ratio (υ)
E-glass	80.22	2.66	22.8	0.23
Lamination resin	3.792	1.19	77.2	3.792

Fig. 1. Gypsum mold for case study

2.2 Manufacturing

Here are the steps to manufacture the glass fiber reinforced composites:

- Jepson Mold preparation: A wooden mold covered from the inside with a soft layer of gypsum with dimensions of (25×35×0.5) cm^3 is used to ensure a flat inner surface. The inside of the mold is coated with PVA wrap to prevent adhesion of the resin and ensure easy removal of the model after solidification.
- Fiberglass arrangement: E-glass fibers are arranged in organized rows, across four consecutive layers within the mold. After each layer, an additional PVA wrap is placed to form the inner bag of the vacuum bagging.
- Preparation of resin mixture and additives: Polymer resin (PMMA in a ratio of 20:80) is mixed with hardening powder at 2% by weight of the resin, as well as Al_2O_3 powder at the desired concentration (2%, 5% or 8%). This mixture provides good cohesion of the fibers and improves the mechanical properties of the sheets.
- Vacuum Bagging Process: The resin mixture is applied to the layers of fibers, fully saturating them. The final overlay is covered with an airtight PVA outer wrap, then the bag is closed. It operates the vacuum pump to be suctioned in two stages: between the inner layer of PVA and the mold to form the casing around the mold. between the layer in which the forming takes place and the outer shell to eject air bubbles and compress the plates. This process continues at a pressure of up to 3000 MPa (as textual) for 45–60 minutes to ensure complete cohesion of the resin with the fibers.
- Curing Process: After the vacuum is finished, the plates are left under the action of pressure and solidification reaction for up to two hours until the crystal formation is complete and the model reaches its final hardness.
- Demolding and finishing: The outer PVA shell open, and the solid sample is removed from the mold. Cutting excess edges with a CNC cutter to obtain precise sheet final dimensions as required (e.g. 25×35 cm for main sheets, or cutting test specimens with dimensions of 165×19–13×3 mm for tensile tests). With these steps, it is safe to manufacture homogeneous

composite sheets, with a smooth surface and free of internal defects, ready for subsequent mechanical and vibratory tests.

2.3 Samples Mechanical Properties

The mechanical properties of the manufactured samples are investigated using a tensile test according to ASTM D3039/D3039M-08 [14]. The test was conducted in the mechanical department at the University of Technology. The results of the tensile test for the manufactured sample are presented in Table 2.

Table 2. Mechanical properties of the manufactured sample.

Sample	E2(MPa)	E2(MPa)	v12	V21	G12(MPa)
8 % Al_2O_3	11209	3521	0.35	0.12	1838
5 % Al_2O_3	8581	3061	0.34	0.117	1776
2 % Al_2O_3	8429	2833	0.37	0.133	1634

2.4 Free Vibration Test

The free vibration test was performed in the mechanical engineering department at the University of Baghdad as follows:

- Sample preparation: Using a single layer composite plate (Orthotropic) with dimensions of (25×35×0.5) cm^3, impregnated with polyester resin with 8% Al_2O_3 powder. Installing the plate under "simply supported" boundary conditions on the test holder.
- Excitation: Using an impact hammer with an ICP force sensor to give a mechanical pulse to the edge of the plate, causing free vibration.
- Measuring Response: Install an accelerometer weighing 3 g at the center of the plate or a point away from the edges, to capture the acceleration signal. Pass the signal through a Brüel & Kjær 2626 charging amplifier, ensuring a frequency range from 0.1 Hz to 30 kHz and an adjustable gain of 0–60 dB. Display the signal on the Digital Oscilloscope DS1102E type, and store the frequency data in flash memory for subsequent analysis.
- Natural frequency extraction: Reading acceleration response peaks represented as waves on an oscilloscope; the natural frequency is extracted from the highest peaks visible in the time or frequency spectrum.
- The free vibration test rig is presented in (Fig. 2).

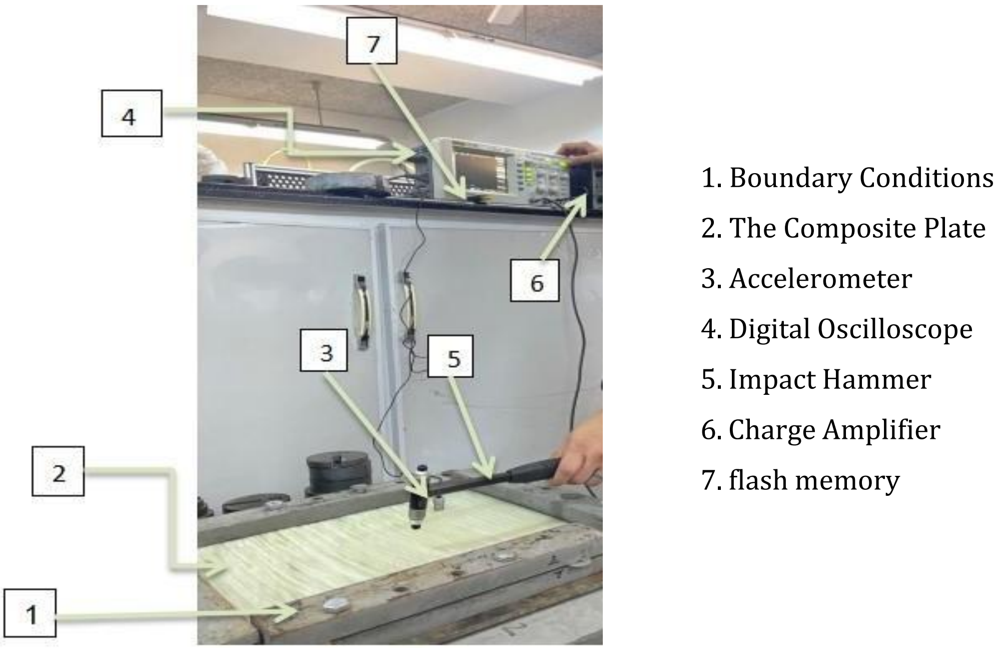

Fig. 2. Rectangular plate vibration test rig

3. Numerical Analysis

This study employed the classical laminated theory CLT as the main assumption; surface mass and Rayleigh–Ritz equations were used to calculate natural frequencies and mode shapes. It was also assumed the following [15]:

- Thin plate (Kirchhoff theory).
- Limits are simply attribution.
- Neglecting the effect of shear (no shear deformation).
- Homogeneous material for each layer.
- No initial stresses or external loads.
- Use sinusoidal functions as shape functions.

Based on the above assumptions, the layer stiffness matrix will be [15]:

$$[Q] = \begin{bmatrix} Q_{11} & Q_{12} & 0 \\ Q_{12} & Q_{22} & 0 \\ 0 & 0 & Q_{66} \end{bmatrix} \tag{1}$$

- $Q_{11} = \frac{E_1}{1-v_{12}\,v_{21}}$= Axial stiffness in the 1-direction.
- $Q_{22} = \frac{E_2}{1-v_{12}\,v_{21}}$= Axial stiffness in the 2-direction.
- $Q_{12} = \frac{v_{12}\,E_1}{1-v_{12}\,v_{21}}$= Coupling stiffness due to Poisson's effect.
- $Q_{66} = G_{12}$: Shear modulus in the plane of the layer (Pa)
- E_1= Young's modulus in fiber direction (Pa)
- E_2= Young's modulus transverse to fibers (Pa)
- v_{12} = Poisson's ratio (strain in direction 2 due to stress in direction 1)
- $v_{21} = \frac{E_2}{E_1} v_{12}$= reciprocal Poisson's ratio by elasticity symmetry

Now the Bending stiffness matrix for the laminate using Classical Laminate Theory (CLT);

$$D = \frac{h^3}{12}\,Q \tag{2}$$

Where; D = Bending stiffness matrix of the laminate (Nm), h = Total thickness of the laminate (m),

Q = Reduced stiffness matrix of the laminate (Pa)

Then, the natural frequency using Rayleigh-Ritz (Simply Supported Plate with sinusoidal shape functions);

$$\omega = \pi^2 \sqrt{\frac{D_{11}}{m}} \left(\left(\frac{m_i}{L_x}\right)^2 + \left(\frac{n_j}{L_y}\right)^2 \right) \tag{3}$$

$$f_{ij} = \frac{\omega}{2\pi} \tag{4}$$

Where; ω = Circular natural frequency (rad/s), f_{ij}= Natural frequency in Hz, D_{11} = Bending stiffness in x-direction from matrix D (Nm) m = Mass per unit area (kg/m^2), L_x = Length of the plate (m), L_y = Width of the plate (m), m_i, n_j = Mode numbers in x and y directions (integer, e.g., 1, 2, 3...).

The mode shape function for a simply supported plate is:

$$w(x,y) = sin\left(\frac{m_i \pi x}{L_x}\right) sin\left(\frac{n_j \pi y}{L_y}\right) \tag{5}$$

Where w(x, y) = Transverse deflection (displacement) at position (x, y) and x, y = Coordinates on the plate surface (m).

The numerical analysis was conducted in two ways: first, using MATLAB code employing the above equations, and second, using ANSYS Workbench 2021 R1, where a (25×35×0.5) cm^3 plate is designed in a CAD (ANSYS DesignModeler). The laminate constituent layers (e.g., 90°, 30°, 45°, 30°, 90° fiber arrangement) and their mechanical properties (E-glass & PMMA) are defined using ANSYS Composite PrepPost ACP (Pre) engineering data. Restrict the four edges of the plate to Simply Supported boundary, i.e.: Vertical movement (Z) is restricted at the edges. Allows rotational motion around the edge axes (X and Y) freely. Two-sided SHELL181 elements (2D shell elements) suitable for composite thin sheet analysis were used, supporting Orthotropic Layers properties and enabling the simulation of stratified grading of glass fibers and polymer resin [14-19]. The average size of the element used is approximately 5×5 mm, to strike a balance between the accuracy of the results and the speed of calculation. The total number of elements is around 4,900, evenly distributed to ensure good coverage of the middle level of the plate, as shown in Fig. 3.

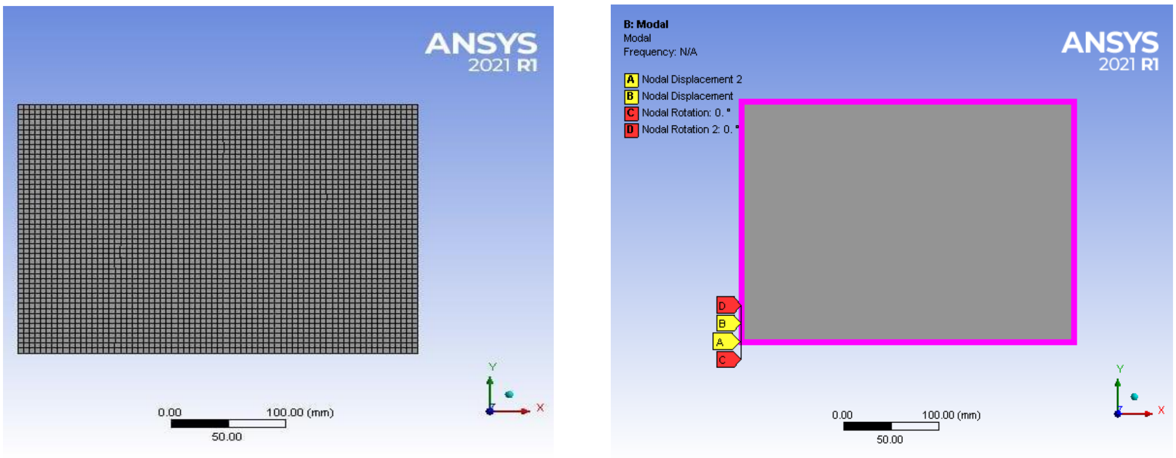

(a) (b)

Fig. 3. a) Mesh type of the modeled sample. b) The boundary conditions: all edges simply supported

3. Results and Discussion

The results of this study were presented Table 3, where the numerical results were presented using ANSYS and MATLAB for the best mechanical properties sample, which is the 8% Al_2O_3 reinforcement (Fig. 4 to Fig. 8) are presenting the first mode results using FEM and analytical solution for the five samples above. Discussion of dynamic performance in terms of the highest natural frequency, where the ranking in sample (4) achieved the highest value of the natural frequency in the first mode (104.51 Hz), which indicates the maximum dynamic rigidity of this arrangement.

In terms of the lowest variation between the models, the sequence in sample (1) was characterized by the least difference between the results of ANSYS and MATLAB (0.45%), which indicates good consistency of analytical and numerical models in this ranking. Complex distributions, the arrangement in sample (3) based on gradually variable angles, showed the greatest variance (8.74%), indicating the boundary of the CLT model in capturing the effects of shearing and morphology in such complex angular combinations.

Table 3. ANSYS and MATLAB natural frequency results

Sample	Mode	ANSYS N.F (Hz)	MATLAB N.F (Hz)	Discrepancy (%)
(1) 90°, 0°, 60°, 0°, 90°	1	100.77	101.23	0.45
	2	176.65	179.78	1.74
	3	317.71	319.39	0.53
	4	330.31	335.68	1.60
	5	401.93	404.92	0.74

(2) 0°, 90°, 45°, 90°, 0°	1	90.79	89.71	1.19
	2	202.56	204.82	1.10
	3	264.58	255.7	3.36
	4	355.54	358.85	0.92
	5	401.17	403.31	0.53
(3) 0°, 60°, 90°, 60°, 0°	1	90.571	99.25	8.74
	2	205.79	225.07	8.57
	3	255.47	258.03	0.99
	4	353.59	396.98	10.93
	5	408.27	427.63	4.53
(4) 90°, 30°, 45°, 30°, 90°	1	104.51	112.07	6.75
	2	177.46	199.86	11.21
	3	309.34	336.14	7.97
	4	348.49	349.65	0.33
	5	409.75	448.29	8.60
(5) 0°, 45°, 90°, 45°, 0°	1	98.61	101.72	3.06
	2	190.31	209	8.94
	3	312.65	328.89	4.94
	4	359.87	373.29	3.60
	5	393.07	406.68	3.35

Mechanically, all five arrangements benefit from an 8% Al_2O_3 boost compared to others, but the stratified arrangement itself does not affect the tensile properties that are tested independently of angular directions. In dynamic terms, rank (4) is the most solid (the highest natural frequency), followed by rank (1), while the rest performed between medium and low values. In terms of typical accuracy, ranking (1) provides the best compatibility between ANSYS and MATLAB, making it ideal for harmonic analysis, while ANSYS alone is preferred for ranking (4) if the focus is on the highest dynamic performance regardless of analytical variation.

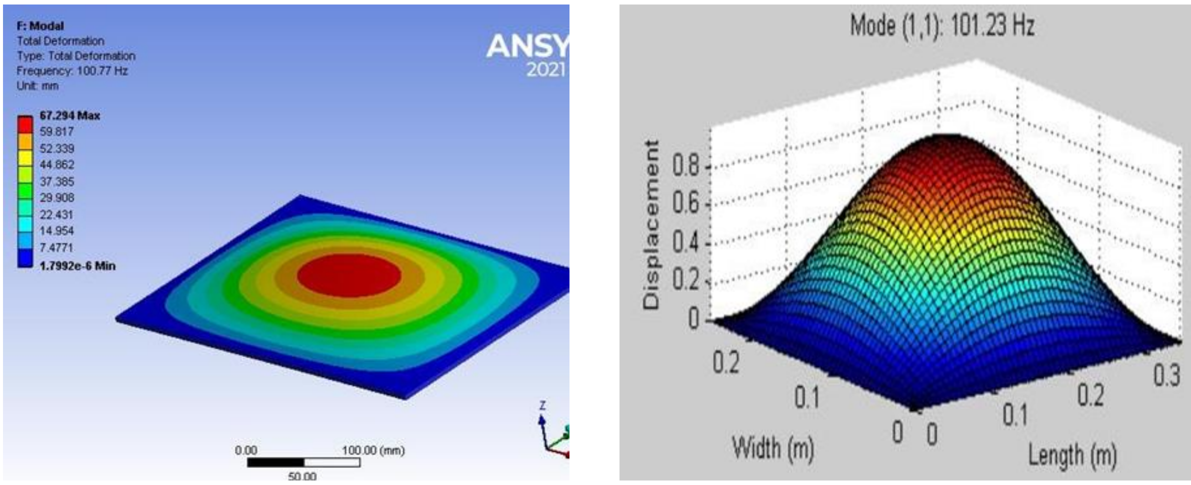

(a) (b)

Fig. 4. Fundamental natural frequency and mode shape of sample 1: a) FEM result, b) analytical result

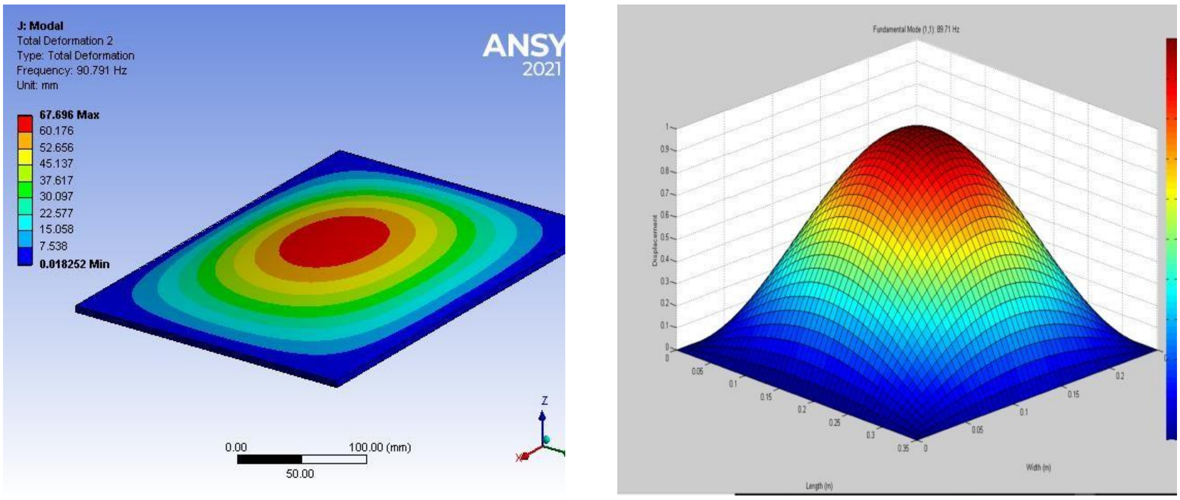

(a) (b)

Fig. 5. Fundamental natural frequency and mode shape of sample 2: a) FEM result, b) analytical result

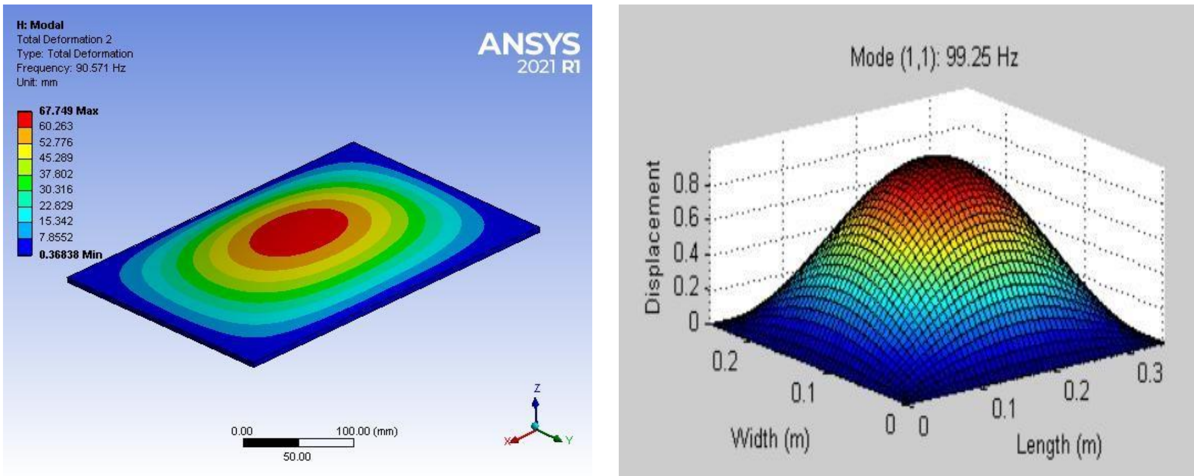

(a) (b)

Fig. 6. Fundamental natural frequency and mode shape of sample 3: a) FEM result, b) analytical result

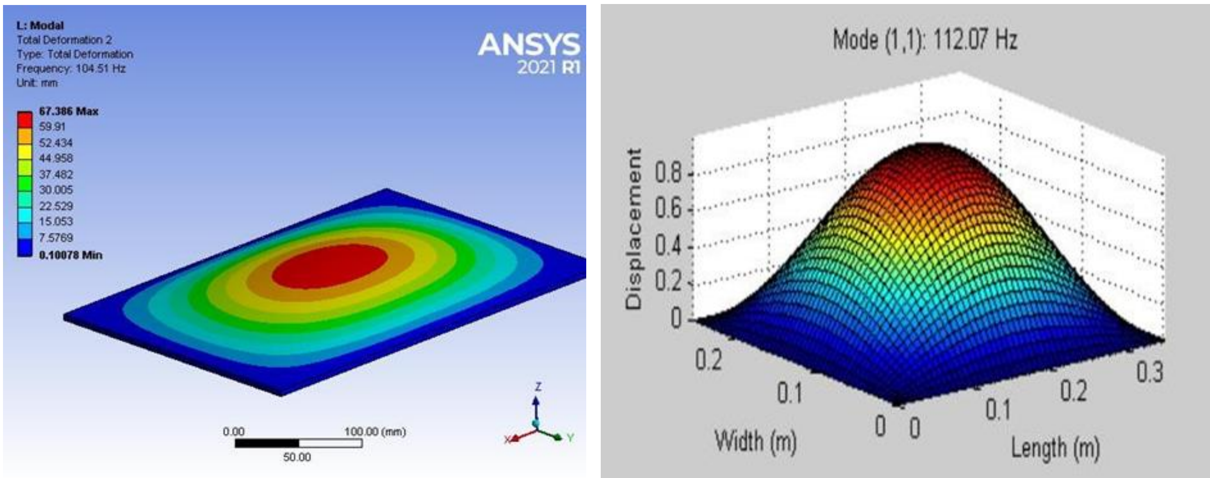

(a) (b)

Fig. 7. Fundamental natural frequency and mode shape of sample 4: a) FEM result, b) analytical result

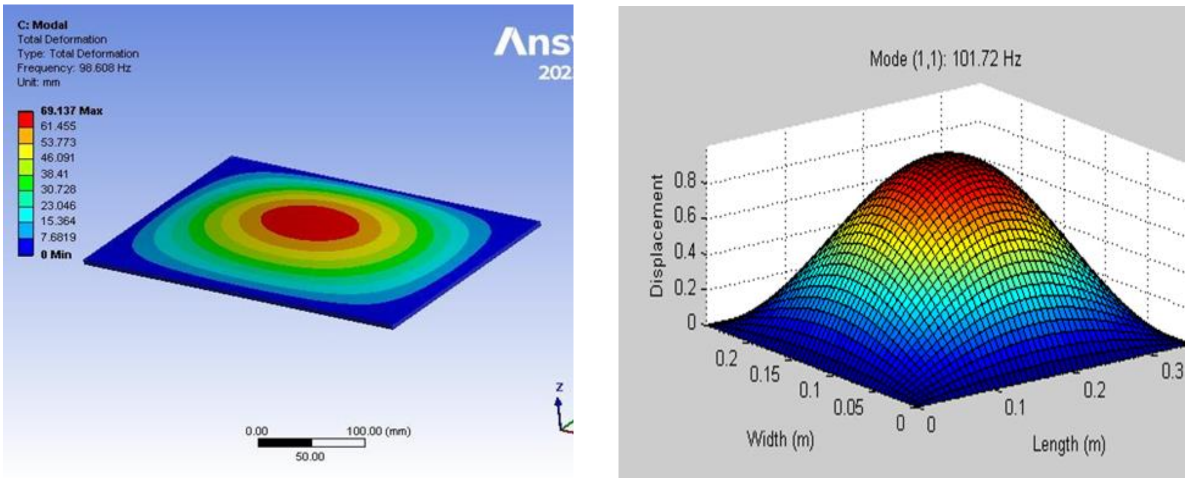

Fig. 8. Fundamental natural frequency and mode shape of sample 5: a) FEM result, b) analytical result

4. Results Validation

The analytical and FEM model analysis was validated using the experimental investigation for a thin composite plate with dimensions of (25×35×0.5) cm^3 of five layers with a stacking sequence of (0°, 90°, 45°, 90°, 0°) as presented in Table 4. In the previous table, the comparison between experimental values, simulated predictions (ANSYS) and analytical calculations (MATLAB) of the natural frequencies of the first five vibration modes of the composite dish (350×250×5 mm^3) with successive layers (0°, 90°, 45°, 90°, 0°) under simple boundary conditions on the edges is shown. The following points can be drawn: the error rate between ANSYS results and experimental values ranges from 1.08% (mode 5) to 2.53% (mode 1), indicating a very good compatibility between simulation and testing. For the MATLAB analytical method, error rates range from 0.03% (mode II) to 3.69% (mode I).

Table 4. Results comparison between experimental, FEM, and analytical.

Mode	FEM Natural Frequency (Hz)	Experimental Natural Frequency (Hz)	Discrepancy (%)	Analytical Natural Frequency (Hz)	Discrepancy %
1	90.79	93.15	2.53	89.71	3.69
2	202.56	204.89	1.14	204.82	0.03
3	264.58	259.23	2.02	255.7	1.36
4	355.54	362	1.78	358.85	0.87
5	401.17	405.56	1.08	403.31	0.55

The MATLAB method is therefore more accurate in modes two to five, while ANSYS slightly outperforms mode one. The reasons for this slight discrepancy may be due to one of the following reasons: In both models, the effect of shear (according to Kirchhoff's theory) and small distortions were neglected, which could lead to differences of up to ~3% in frequencies. The ideal simple edge model is slightly different from experimental reality (where there may be slight friction or ripple in the stabilization of the sample). The effect of the mass of the sensor (accelerator) and the properties of the actual material of the resin may add a small deviation in the measured frequencies.

5. Conclusions

This study investigated the free vibration behavior of orthotropic composite plates reinforced with Al_2O_3 particles, addressing the critical need for lightweight, high-stiffness materials in aerospace and automotive applications. The research employed a comprehensive approach combining analytical (CLT), numerical (FEM), and experimental methods to analyze five different fiber stacking sequences with varying Al_2O_3 content (2%, 5%, 8%), the following conclusions can be drawn:

- Particle Enhancement (Al_2O_3): 8% reinforced samples showed the highest tensile strength, Young's modulus, and absorption energy compared to 2% and 5% samples, demonstrating the feasibility of increasing the particle content to improve the mechanical properties of the composite.
- Dynamic performance and optimal fiber arrangement: The 90°, 30°, 45°, 30°, 90° ranking achieved the highest first natural frequency (104.51 Hz in ANSYS), demonstrating the maximum dynamic rigidity between the structures studied. In contrast, the 90°, 0°, 60°, 0°, 90° arrangement provides the best analytical–numerical compatibility (0.45% difference), ideal for initial calibration and rapid analysis.
- Accuracy of analytical and numerical models: At identical structures (e.g. 90°, 0°, 60°, 0°, 90°
- and 0°, 90°, 45°, 90°, 0°), the CLT-based MATLAB method recorded accuracy superiority (errors <1.2%), with excellent compatibility with experimental and ANSYS numerical results. The greater the complexities of the angles (0°, 60°, 90°, 60°, 0° and 90°, 30°, 45°, 30°, 90°), the higher the contrast ratio (up to ~11%), which requires numerical simulation in ANSYS to give more reliable results.

The recommendations for future works are:

- Include shear effects and analysis of nonlinear bends to optimize the CLT model.
- Study the distribution of particles within the layer and their homogeneity to reduce variations between models.
- To examine the effect of increasing the ratio of Al_2O_3 above 8% and to evaluate the effect of the resulting density on dynamic and mechanical performance.
- Based on these results, it is recommended to use an 8% Al_2O_3 sample with a 90°–30°–45°–30°–90° order when maximum dynamic rigidity is required, with a 90°–0°–60°–0°–90° order in the first analytical analyses to ensure high compatibility of results.

References

[1] El-Kady EY, Mahmoud TS, El-Betar AA, Abdel-Aziz M. Dynamic behaviour of cast A356/Al2O3 aluminum metal matrix nanocomposites. Mater Sci Appl. 2012 Nov 27;3(11):815-20. https://doi.org/10.4236/msa.2012.311118

[2] Al-Shammari MA, Abdullah SE. Stiffness to Weight Ratio of Various Mechanical and Thermal Loaded Hyper Composite Plate Structures. IOP Conf Ser Mater Sci Eng. 2018 Nov;433(1):012051. https://doi.org/10.1088/1757-899X/433/1/012051

[3] Al-Waily M, Al-Shammari MA. Theoretical and Numerical Vibration Investigation Study of Orthotropic Hyper Composite Plate Structure. Int J Mech Mechatron Eng. 2014.

[4] Merdaci S, Adda HM, Hakima B, Dimitri R, Tornabene F. Higher-Order Free Vibration Analysis of Porous Functionally Graded Plates. J Compos Sci. 2021 Nov;5(11):305. https://doi.org/10.3390/jcs5110305

[5] Navaneeth IM, Poojary S, Chandrashekar A, Razak A, Hasan N, Almohana AI. Damped Free Vibration Analysis of Woven Glass Fiber-Reinforced Epoxy Composite Laminates. Adv Mater Sci Eng. 2022 Jul;2022:1-13. https://doi.org/10.1155/2022/6980996

[6] Al-Shablle M, Njim EK, Jweeg MJ, Al-Waily M. Free vibration analysis of composite face sandwich plate strengthens by Al2O3 and SiO2 nanoparticles materials. Diagnostyka. 2023 Apr;24(2):1-9. https://doi.org/10.29354/diag/162580

[7] Vasara D, Khare S, Sharma HK, Kumar R. Free vibration analysis of functionally graded porous circular and annular plates using differential quadrature method. Forces Mech. 2022 Dec;9:100126. https://doi.org/10.1016/j.finmec.2022.100126

[8] Saidi H, Sahla M. Vibration analysis of functionally graded plates with porosity composed of a mixture of Aluminum (Al) and Alumina (Al2O3) embedded in an elastic medium. Frat ed Integrità Strutturale. 2019 Aug;13(50):286-99. https://doi.org/10.3221/IGF-ESIS.50.24

[9] Venkatalakshmi N, Krishnabhaskar K, Meerasaheb K. Free Vibration Analysis of Simply Supported and Clamped Functionally Graded Rectangular Plate Using Coupled Displacement Field Method. Mech Adv Compos Struct. 2025;12(1):73-84.

[10] Li H, Liu N, Pang F, Du Y, Li S. An Accurate Solution Method for the Static and Vibration Analysis of Functionally Graded Reissner-Mindlin Rectangular Plate with General Boundary Conditions. Shock Vib. 2018 Jan;2018(1). https://doi.org/10.1155/2018/4535871

[11] Tavadi AR, et al. Experimental analysis of mechanical properties and FTIR analysis of areca fiber-reinforced epoxy composites incorporating Al2O3. J Ind Text. 2025 Dec;55. https://doi.org/10.1177/15280837241313217

[12] Han Y, Shi Z, Hua C, Sang Y, Gao H, Wang Y. Analysis of mechanical and vibration properties of carbon fiber reinforced polymer matrix composites with SiO2 / Al2O3 micron particles. Polym Compos. 2025 Apr;46(5):4800-14. https://doi.org/10.1002/pc.29278

[13] Mawardi I, Razak H, Akadir Z, Jaya RP. The effect of containing Al2O3 microparticles in different matrix polymers on properties of pineapple fiber-reinforced composites. Frat ed Integrità Strutturale. 2023 Dec;18(67):94-107. https://doi.org/10.3221/IGF-ESIS.67.07

[14] ASTM International. ASTM D3039/D3039M-08: Test Method for Tensile Properties of Polymer Matrix Composite Materials. West Conshohocken, PA: ASTM International; 2008.

[15] Reddy JN. Theory and Analysis of Elastic Plates and Shells. 2nd ed. Boca Raton: CRC Press; 2006. https://doi.org/10.1201/9780849384165

[16] Emad A, Idan MM. Numerical analysis of low-velocity impact behavior on composite materials. Pollack Period. 2025 Mar;20(1):95-101. https://doi.org/10.1556/606.2024.01148

[17] Hussein A, Abbas AWN, Alshubber HA. Applying the photo-elasticity method to study teeth stresses in a variety of spur gears. Pollack Period. 2025 Apr. https://doi.org/10.1556/606.2024.01248

[18] Burlayenko VN, Sadowski T. Free vibrations and static analysis of functionally graded sandwich plates with three-dimensional finite elements. Meccanica. 2020 Apr;55(4):815-32. https://doi.org/10.1007/s11012-019-01001-7

[19] Ganesh S, Kumar KS, Mahato PK. Free Vibration Analysis of Delaminated Composite Plates Using Finite Element Method. Procedia Eng. 2016;144:1067-75. https://doi.org/10.1016/j.proeng.2016.05.061

[20] Pingulkar P, Suresha B. Free Vibration Analysis of Laminated Composite Plates Using Finite Element Method. Polym Polym Compos. 2016 Sep;24(7):529-38. https://doi.org/10.1177/096739111602400712

[21] Shakouri M. Free vibration analysis of functionally graded rotating conical shells in thermal environment. Compos B Eng. 2019 Apr;163:574-84. https://doi.org/10.1016/j.compositesb.2019.01.007